SUPPLEMENTAL EXPERIMENTAL PROCEDURES

Cell culture

All cancer cell lines were obtained from ATCC except the Moser colon cancer cell line, which were a gift from Dr. Bruce Spiegelman. All cell lines were cultured in Dulbecco's Modified Eagle's Medium with 10% fetal bovine serum. Mouse PEPCK cDNA (mPEPCK1) was a gift from Dr. Richard Hanson (Case Western Reserve). mPEPCK1 was subcloned into the pMSCVpuro retroviral vector (Clontech). pMSCV and PEPCK retrovirus were generated and transduced into HT29 cells as previously described (Drori et al., 2005; Girnun et al., 2007). Stable cells were generated by selecting in 2 ug/mL puromycin and overexpression of PEPCK confirmed by RTPCR and western blotting. Non-target control and validated shRNAs against human PEPCK in a pLKO.1 lentiviral backbone were obtained from Sigma. Lentivirus was produced as per manufactures directions and Colo205 and Moser cells transduced and selected for stable pools using 2 μg/mL or 10 μg/mL puromycin, respectively. Western blotting confirmed knockdown of PEPCK. Phosphoenolpyruvate and oxaloacetate levels were determined using a kit from Biovision's according to manufactures direction.

Analysis of PEPCK expression in human tumors:

Expression profiling array data from a published study was used to analyze the PEPCK expression in multiple tumors (Ramaswamy et al., 2001). Normalized gene expression values were log2 transformed, and the sample replicate values were averaged. The relative PEPCK expression for each tumor cell type was calculated by subtracting the median expression value, and plotted as a bar graph. The CBioPortal was used to analyze PEPCK expression in 195 tumors (Cerami et al., 2012; Gao et al., 2013). Immunohistochemistry was performed on a commercial TMA by the Stony Brook Histopathology Core. The TMA was deparaffinized and antigen retrieval performed in citrate buffer [20 mmol/l (pH 6.0)] at 120^{o} C for 10 min in a Decloaking Chamber. Sections were incubated using rabbit polyclonal anti-PCK1

[HPA0006507] primary antibody (Sigma Life Science) diluted 1:100, followed by detection with an avidin-biotin based system (Vectastain ABC) and development with 3,3′-diaminobenzidine. After dilute hematoxylin counterstaining, sections were dehydrated and coverslipped for bright-field microscopy. Negative controls were performed by substituting the primary antibody solution with TBST buffer.

Immunoblotting

Cells and tissues were homogenized in RIPA buffer (Cell Signaling Technology) with phosphatase and protease inhibitor cocktails added. Proteins were separated on a 4-12% SDS polyacrylamide gel, transferred to nitrocellulose and probed with antibodies against mouse and human PEPCK (Abnova) and PEPCK (Cayman Chemical). Proteins were also immunoblotted for total 4EPB1 (#9644), p-4EBP1$^{Thr37/56}$(#2588), S6 Ribosomal Protein (#2217), P-S6 Ribosomal protein$^{Ser249/244}$#2215), p70 S6 Kinase (#9202), and Phospho-p70 S6 Kinase^{Thr389} (#9234) (Cell Signaling) and actin as a loading control (Sigma). HRP conjugated secondary antibodies (Jackson Immunoresearch) were used and proteins visualized using ECL.

Immunofluorescence

Colo205 NTshRNA and shPEPCK cell lines were grown on a glass chamber slides. Slides were fixed with 4% formaldehyde and subjected to immunofluorescence staining. Primary antibodies used were LAMP2 (1:100; Abcam, ab25631) and mTOR (1:400; cell signaling, #2983). Slides were cover slipped and images captured using an Olympus Fluoview FV1000 confocal microscope. Slides were observed using a 60x Plan Apo N 1.42 oil immersion objective.

Growth Assay

Cells were seeded at 10,000-25,000 cells/well in 6-well plates, and allowed to grow at 37°C, 5% CO_2. At the indicated number of days, cells were trypsinized and counted using a hemocytometer (Reichter) or Countess Automated Cell Counter. For clonogenic assay, cells were seeded at 2000-5000 cells/well in 6-well plates and allowed to grow at 37°C, 5% CO_2. At the end of ~2 weeks cells were fixed and stained using crystal violet and colony counting performed using ImageJ. For treatment studies, cells were seeded at 50,000-100,000 cells/well in 6 well plates and then treated with indicated doses of drugs for up to 3 days. For rapamycin treatment, cells were seeded overnight and then treated with 10 nM rapamycin for 48 hr, at which point cells were counted using a Countess Automated Cell Counter.

Animal work

Animal experiments were performed according to procedures approved by the University of Maryland, Baltimore IACUC. $2X10^6$ HT29 pMSCV, HT29-PEPCK, Colo205-NTshRNA and Colo205-PEPCKshRNA cells were inoculated into the flank of 6-week old SCID mice. Tumors were measured and tumor size determined as previously described (Girnun et al., 2007). Mice were injected IP with 50 mg/kg BrdU 3 hr prior to euthanasia. Tumors were removed and either snap frozen for protein and RNA analysis, or fixed in buffered formaldehyde (Fisher Scientific) for paraffin embedding and histopathology and immunohistochemistry. Sections were stained for BrdU incorporation according to manufactures directions (Roche). For treatment experiments, xenografts were established as described above but in nude mice. Once tumors became palpable, mice were administered 10 mg/kg PEPCK inhibitor every other day and tumors measured for an additional 10 days.

Glucose and glutamine uptake studies

Cells were seeded in a 6 well plate and serum deprived overnight. Cells were then treated with 2μCi of 2-deoxy-D-^{14}C-[U]-glucose (GE Amersham) in complete media for 6 hours, washed with PBS and then harvested. Glucose uptake was determined using liquid scintillation counting. For glutamine uptake experiments, cells were cultured in complete media for 2 days and changed to media containing 1μM ^{14}C-[U]-glutamine for 5 min. Cells were washed with PBS, harvested and glutamine uptake determined using LSC.

^{13}C tracer studies

Cells were seeded in triplicate into 100mm dishes and allowed to grow overnight. [U5-$^{13}C_5$]glutamine and [U6-$^{13}C_6$]-glucose (>99% purity and 99% isotope enrichment for each carbon position; Cambridge Isotope Labs) were used as tracers since they provide excellent analysis of overall central carbon metabolism and in particular the TCA cycle (Metallo et al., 2009). Cells were incubated for 36 hours in a 1:1 ratio of ^{13}C tracer to naturally occurring ^{12}C tracer. Briefly, following glucose or glutamine treatment, culture medium was collected and cells were washed twice in PBS, after which cell pellets were harvested, Specific extractions and analysis were performed as previously described and below (Bhalla et al., 2011; Boren et al., 2001; Boros et al., 1997; Mullen et al., 2012; Singh et al., 2013). Lactate was extracted from cell culture media by ethylene chloride after acidification with HCl, derivatized to its propylamine-heptafluorobutyrate ester form, and applied to the column. The *m/z* 328 (carbons 1–3 of lactate; chemical ionization) were monitored for positional mass isotopomer determination. Fatty acids were extracted by saponification of Trizol cell extracts after removal of the RNA containing supernatant with 30% KOH and 100% ethanol using petroleum ether. Fatty acids were then converted to their methylated derivatives using 0.5 N methanolic-HCl. Palmitate and myristate were monitored at *m/z* 270 and *m/z* 242, respectively. The enrichment of acetyl units and the

synthesis of new lipid fraction were determined using the mass isotopomers of palmitate with the enrichment of ^{13}C-labeled acetyl units used to reflect synthesis, elongation, and desaturation of the new lipid fraction as determined by mass isotopomer distribution analysis (MIDA) (Lee et al., 1995). RNA ribose was isolated by acid hydrolysis of cellular RNA after Trizol purification of cell extracts. Ribose was isolated from RNA and derivatized to its aldonitrile acetate form using hydroxylamine in pyridine with acetic anhydride (Supelco) before mass spectral analyses as previously described (Lee et al., 1998). The ion cluster was monitored around the *m/z* 256 (carbons 1–5 of ribose; chemical ionization), *m/z* 217 (carbons 3–5 of ribose), and *m/z* 242 (carbons 1–4 of ribose; electron impact ionization) to determine concentration and positional distribution of ^{13}C in ribose as previously described (Boros et al., 2005; Boros et al., 1997; Boros et al., 2000; Lee et al., 1998; Liu et al., 2010; Vizan et al., 2005). TCA cycle intermediates, glycolytic intermediates and ribose were determined via an alternate method. Cells were cultured in media containing glutamine and only ^{13}C labeled glucose or glucose and only ^{13}C labeled glutamine for 24 hr. Cells were washed and then scraped into 50% methanol:water, snap frozen three times, spun down and supernatant isolated. The supernatant was then dried down and methoximated and derivatized as previously described (Mullen et al., 2012). Citrate was monitored at 465-471, succinate at m/z 247-251, fumarate at m/z 245-249, malate at m/z 335-339, glutamate at m/z 348-353, and αketoglutarate at m/z 304-309. Glucose 6 phosphate was monitored at m/z 357-359, lactate at m/z 219-222, phosphoenolpyruvate at m/z 369-372, and pyruvate at m/z 174-177. Ribose was monitored at 217-220 m/z, which includes carbons 3, 4 and 5. ISOCOR was used to normalize data to an internal standard. For studies showing relative abundance of 13C labeled metabolites (and their isotopomers), 10 nmoles of adonitol was used as an internal standard.

Gas Chromatography/Mass Spectrometry (GC/MS): Mass spectral data were obtained on the HP5973 mass selective detector connected to an HP6890 gas chromatograph. The settings

are as follows: GC inlet 230 ^{o}C, transfer line 280 ^{o}C, MS source 230 ^{o}C MS Quad 150 ^{o}C. An HP-5 capillary column (30m length, 250μm diameter, 0.25μm film thickness) was used for glucose, ribose, and lactate analysis. A Bpx70 column (25m length, 220μm diameter, 0.25μm film thickness, SGE Incorporated, Austin, TX) was used for fatty acid analysis with specific temperature programming for each compound studied.

ECAR Measurements

Cellular glycolytic rate, represented as ECAR, was measured using a Seahorse Biosciences XF96 analyzer (North Billerica, MA). Stable knockdown cells were plated on a Seahorse Biosciences 96 well plate and incubated for 16 hrs and then assayed with glycolytic stress test kit (Seahorse Biosciences, 103020-100). For Rapamycin experiments, cells were pretreated in the Seahorse biosciences 96 well plate overnight and assayed with 10 nM Rapamycin.

Bhalla, K., Hwang, B.J., Dewi, R.E., Ou, L., Twaddel, W., Fang, H.B., Vafai, S.B., Vazquez, F., Puigserver, P., Boros, L.*, et al.* (2011). PGC1alpha Promotes Tumor Growth by Inducing Gene Expression Programs Supporting Lipogenesis. Cancer Res *71*, 6888-6898.
Boren, J., Cascante, M., Marin, S., Comin-Anduix, B., Centelles, J.J., Lim, S., Bassilian, S., Ahmed, S., Lee, W.N., and Boros, L.G. (2001). Gleevec (STI571) influences metabolic enzyme activities and glucose carbon flow toward nucleic acid and fatty acid synthesis in myeloid tumor cells. J Biol Chem *276*, 37747-37753.
Boros, L.G., Lerner, M.R., Morgan, D.L., Taylor, S.L., Smith, B.J., Postier, R.G., and Brackett, D.J. (2005). [1,2-13C2]-D-glucose profiles of the serum, liver, pancreas, and DMBA-induced pancreatic tumors of rats. Pancreas *31*, 337-343.
Boros, L.G., Puigjaner, J., Cascante, M., Lee, W.N., Brandes, J.L., Bassilian, S., Yusuf, F.I., Williams, R.D., Muscarella, P., Melvin, W.S.*, et al.* (1997). Oxythiamine and dehydroepiandrosterone inhibit the nonoxidative synthesis of ribose and tumor cell proliferation. Cancer Res *57*, 4242-4248.
Boros, L.G., Torday, J.S., Lim, S., Bassilian, S., Cascante, M., and Lee, W.N. (2000). Transforming growth factor beta2 promotes glucose carbon incorporation into nucleic acid ribose through the nonoxidative pentose cycle in lung epithelial carcinoma cells. Cancer Res *60*, 1183-1185.
Cerami, E., Gao, J., Dogrusoz, U., Gross, B.E., Sumer, S.O., Aksoy, B.A., Jacobsen, A., Byrne, C.J., Heuer, M.L., Larsson, E.*, et al.* (2012). The cBio cancer genomics portal: an open platform for exploring multidimensional cancer genomics data. Cancer Discov *2*, 401-404.

Drori, S., Girnun, G.D., Tou, L., Szwaya, J.D., Mueller, E., Xia, K., Shivdasani, R.A., and Spiegelman, B.M. (2005). Hic-5 regulates an epithelial program mediated by PPARgamma. Genes Dev *19*, 362-375.
Gao, J., Aksoy, B.A., Dogrusoz, U., Dresdner, G., Gross, B., Sumer, S.O., Sun, Y., Jacobsen, A., Sinha, R., Larsson, E.*, et al.* (2013). Integrative analysis of complex cancer genomics and clinical profiles using the cBioPortal. Science signaling *6*, pl1.
Girnun, G.D., Naseri, E., Vafai, S.B., Qu, L., Szwaya, J.D., Bronson, R., Alberta, J.A., and Spiegelman, B.M. (2007). Synergy between PPARgamma ligands and platinum-based drugs in cancer. Cancer Cell *11*, 395-406.
Lee, W.N., Boros, L.G., Puigjaner, J., Bassilian, S., Lim, S., and Cascante, M. (1998). Mass isotopomer study of the nonoxidative pathways of the pentose cycle with [1,2-13C2]glucose. Am J Physiol *274*, E843-851.
Lee, W.N., Byerley, L.O., Bassilian, S., Ajie, H.O., Clark, I., Edmond, J., and Bergner, E.A. (1995). Isotopomer study of lipogenesis in human hepatoma cells in culture: contribution of carbon and hydrogen atoms from glucose. Analytical biochemistry *226*, 100-112.
Liu, H., Huang, D., McArthur, D.L., Boros, L.G., Nissen, N., and Heaney, A.P. (2010). Fructose induces transketolase flux to promote pancreatic cancer growth. Cancer Res *70*, 6368-6376.
Metallo, C.M., Walther, J.L., and Stephanopoulos, G. (2009). Evaluation of 13C isotopic tracers for metabolic flux analysis in mammalian cells. J Biotechnol *144*, 167-174.
Mullen, A.R., Wheaton, W.W., Jin, E.S., Chen, P.H., Sullivan, L.B., Cheng, T., Yang, Y., Linehan, W.M., Chandel, N.S., and DeBerardinis, R.J. (2012). Reductive carboxylation supports growth in tumour cells with defective mitochondria. Nature *481*, 385-388.
Ramaswamy, S., Tamayo, P., Rifkin, R., Mukherjee, S., Yeang, C.H., Angelo, M., Ladd, C., Reich, M., Latulippe, E., Mesirov, J.P.*, et al.* (2001). Multiclass cancer diagnosis using tumor gene expression signatures. Proc Natl Acad Sci U S A *98*, 15149-15154.
Singh, A., Happel, C., Soumen, K.M., Acquaah-Mensah, G., Carratero, J., Kumar, S., Nasipuri, P., Krausz, K.W., Wakabayashi, N., Dewi, R.*, et al.* (2013). Nrf2 regulates miR-1 and miR-206 to drive tumorigenesis. Journal of Clinical Investigation *In Press*.
Vizan, P., Boros, L.G., Figueras, A., Capella, G., Mangues, R., Bassilian, S., Lim, S., Lee, W.N., and Cascante, M. (2005). K-ras codon-specific mutations produce distinctive metabolic phenotypes in NIH3T3 mice [corrected] fibroblasts. Cancer Res *65*, 5512-5515.

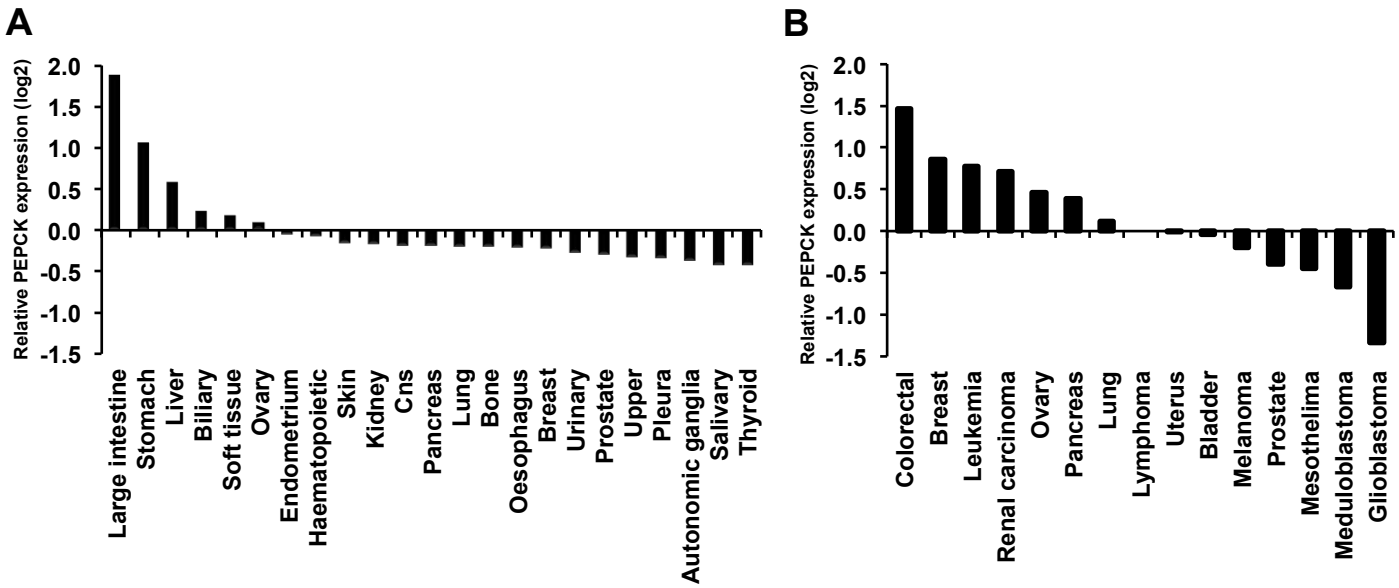
A
Relative PEPCK expression (log2)
2.0
1.5
1.0
0.5
0.0
-0.5
-1.0
-1.5
Large intestine
Stomach
Liver
Biliary
Soft tissue
Ovary
Endometrium
Haematopoietic
Skin
Kidney
Cns
Pancreas
Lung
Bone
Oesophagus
Breast
Urinary
Prostate
Upper
Pleura
Autonomic ganglia
Salivary
Thyroid
B
Relative PEPCK expression (log2)
Colorectal
Breast
Leukemia
Renal carcinoma
Ovary
Pancreas
Lung
Lymphoma
Uterus
Bladder
Melanoma
Prostate
Mesothelima
Medulloblastoma
Glioblastoma

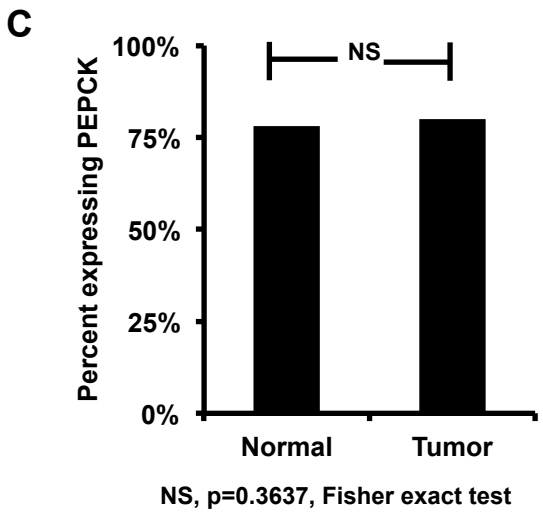
C
Percent expressing PEPCK
100%
75%
50%
25%
0%
NS
Normal
Tumor
NS, p=0.3637, Fisher exact test

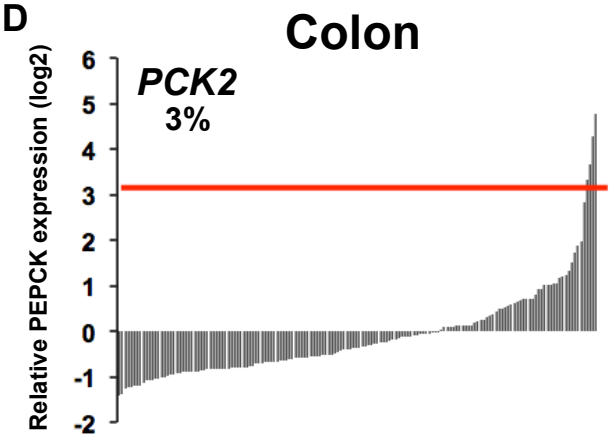
D
Colon
PCK2
3%
Relative PEPCK expression (log2)
6
5
4
3
2
1
0
-1
-2

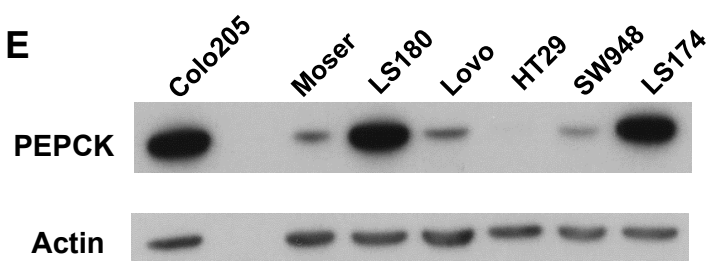
E
Colo205
Moser
LS180
Lovo
HT29
SW948
LS174
PEPCK
Actin

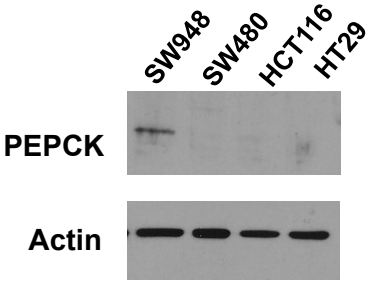
SW948
SW480
HCT116
HT29
PEPCK
Actin

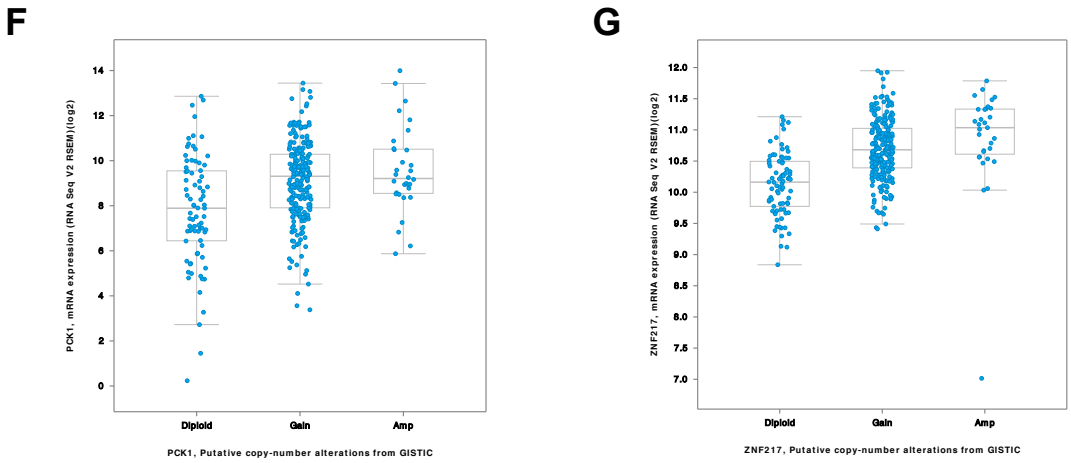

Figure S1, related to Figure 1. Expression of PEPCK in normal tissue, tumor tissue and cell lines.

A) Expression analysis of PEPCK expression in cancer cell lines derived from different tissues (TCGA database).

B) A) Expression analysis of PEPCK expression in cancer cell lines derived from different tissues (Ramaswamy et al. 2001)

C) TMA analysis of PEPCK showing the percent of sections expressing low to high PEPCK.

D) PEPCK2 (*PCK2*) in colon derived tumors analyzed using the TCGA database

E) Expression of PEPCK protein in a collection of colon derived cancer cell lines.

F) 20q13 copy number compared to gene expression for PEPCK mRNA versus copy number using cBioPortal.

PEPCK expression in ovarian cancer, n=158. *z=2,* Data analyzed using the TCGA database

G) 20q13 copy number compared to gene expression for ZNF217 mRNA versus copy number using cBioPortal

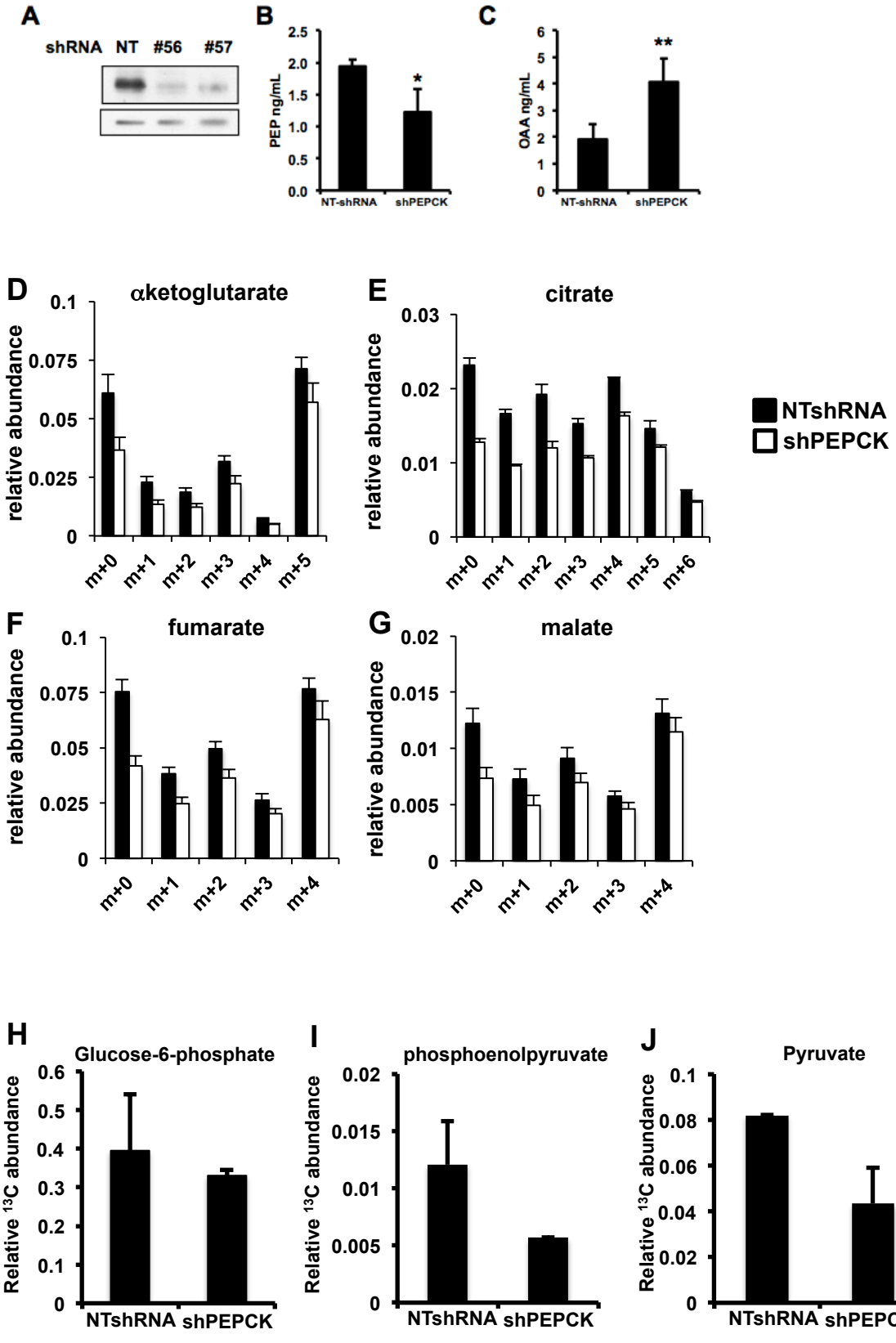
A
shRNA NT #56 #57
B
PEP ng/mL
NT-shRNA
shPEPCK
C
OAA ng/mL
NT-shRNA
shPEPCK
D
αketoglutarate
relative abundance
m+0 m+1 m+2 m+3 m+4 m+5
E
citrate
relative abundance
m+0 m+1 m+2 m+3 m+4 m+5 m+6
NTshRNA
shPEPCK
F
fumarate
relative abundance
m+0 m+1 m+2 m+3 m+4
G
malate
relative abundance
m+0 m+1 m+2 m+3 m+4
H
Glucose-6-phosphate
Relative 13C abundance
NTshRNA shPEPCK
I
phosphoenolpyruvate
Relative 13C abundance
NTshRNA shPEPCK
J
Pyruvate
Relative 13C abundance
NTshRNA shPEPCK

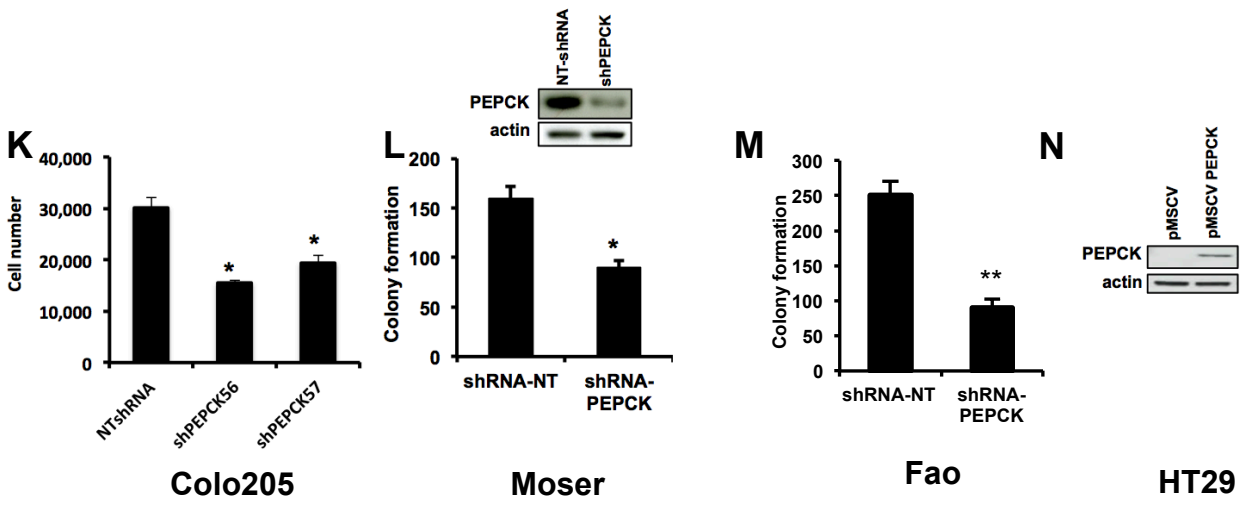

Figure S2, related to Figure 2. PEPCK regulates the TCA cycle and cell proliferation.
A) Knockdown of PEPCK in Colo205 CRC cell line with distinct shRNAs.
B) PEP and C) OAA levels in cells with reduced PEPCK expression. PEPCK regulates cell proliferation. Isotopomer analysis for
^{13}C mass isotopomers for **D**) α−ketoglutarate, **E**) citrate **F**) fumarate, and **G**)malate from NTshRNA and shPEPCK Colo205 cells
Relative ^{13}C abundance for **H**) Glucose 6 phosphate, **I)** phosphoenolpyruvate, and **J**) pyruvate from NTshRNA and shPEPCK Colo205 cells
K) Cell number after 5 days in non-target shRNA Colo205 and Colo205s with different shRNAs against PEPCK.
L) Clonogenic assay of Moser CRC cells with PEPCK shRNA based knockdown. Inset; Knockdown of PEPCK in Moser cells.
M) Clonogenic assay of Fao hepatoma cells with PEPCK shRNA based knockdown.
N) Expression of PEPCK in HT29 cells with exogenous PEPCK.
N=3 ± SD, *p < 0.05, **p < 0.01.

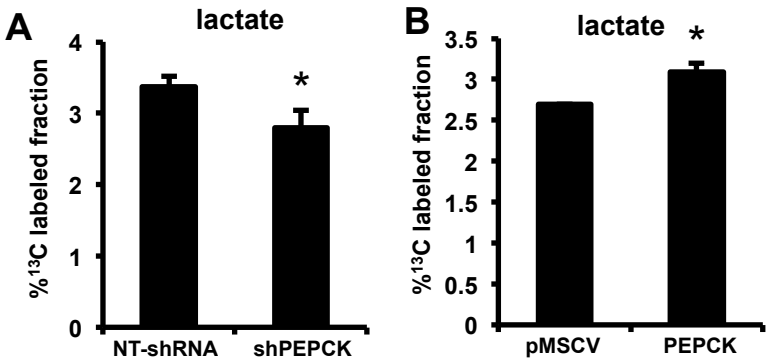
A
lactate
%13C labeled fraction
4
3
2
1
0
*
NT-shRNA
shPEPCK
B
lactate
*
%13C labeled fraction
3.5
3
2.5
2
1.5
1
0.5
0
pMSCV
PEPCK

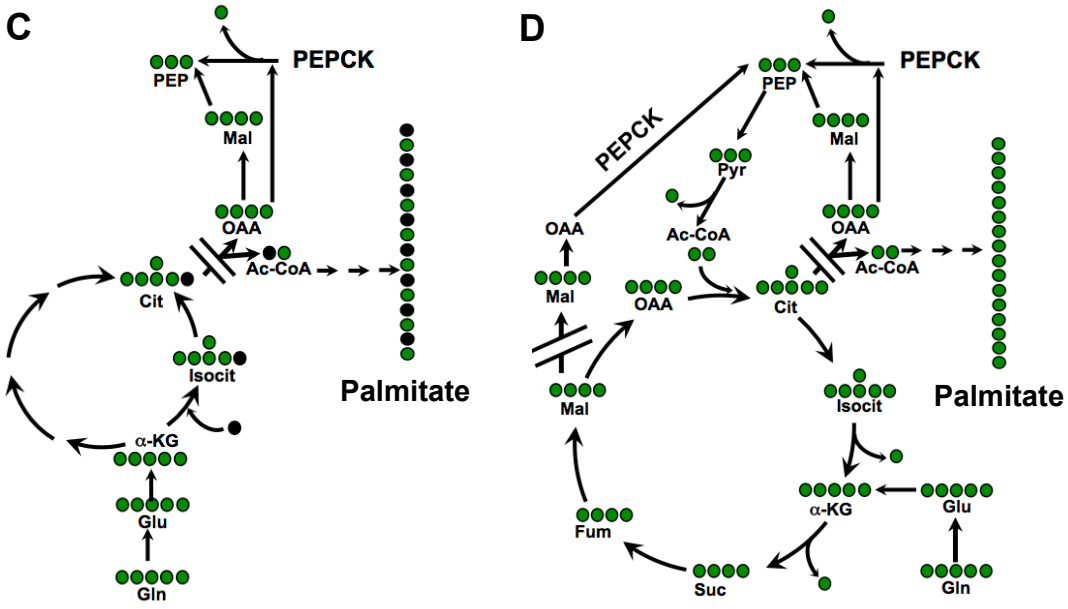
C
PEPCK
PEP
Mal
OAA
Ac-CoA
Cit
Isocit
α-KG
Glu
Gln
Palmitate
D
PEPCK
PEP
PEPCK
Pyr
Mal
OAA
Ac-CoA
OAA
Ac-CoA
Mal
OAA
Cit
Mal
Isocit
Palmitate
α-KG
Glu
Fum
Suc
Gln

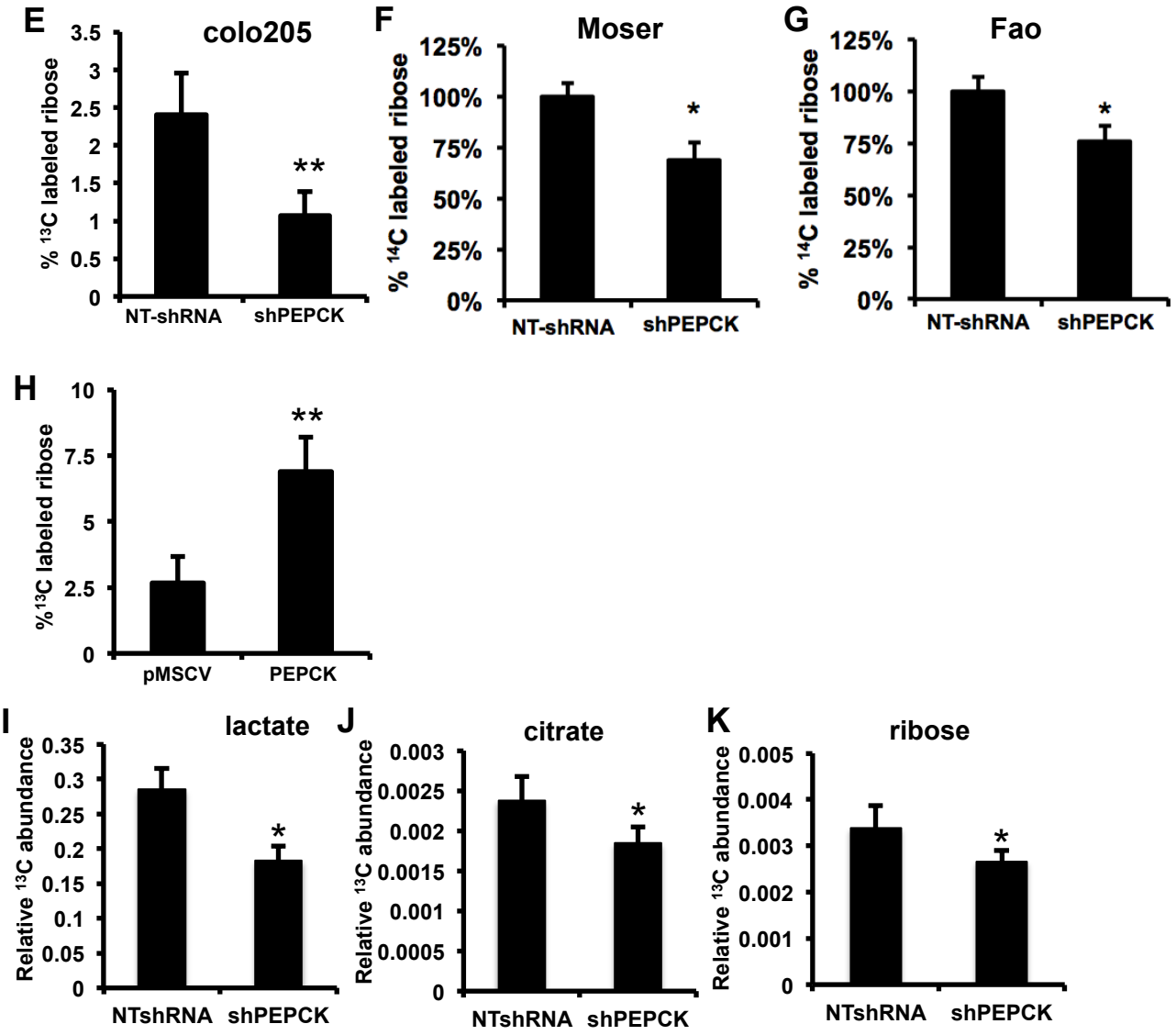

Figure S3, related to Figure 4. PEPCK promotes glutamine utilization towards lipogenesis and ribose synthesis .

A) Fractional labeling of ^{13}C lactate derived from [U5]-glutamine in Colo205 cells with non target shRNA and PEPCK knockdown or **B**) HT29 cells with empty vector or overexpressing PEPCK. Expressed as a percent of total pool.

C) Schematic for labeling of palmitate via reductive carboxylation of glutamine

D) Schematic for labeling of palmitate via classic flow of the TCA cycle.

E) Fractional labeling of ^{13}C ribose derived from [U5]-glutamine in Colo205 cells with non target shRNA and PEPCK knockdown. Expressed as a percent of total pool.

^{14}C labeled RNA/ribose following incubation of non target shRNA and PEPCK knockdown F) Moser or G) Fao cells with ^{14}C glutamine.

H) Fractional labeling of ^{13}C ribose derived from [U5]-glutamine in HT29 cells with empty vector or overexpressing PEPCK. Expressed as a percent of total pool.

N=3 ± SD, *p < 0.05, **p < 0.01.

Relative abundance of ^{13}C labeled **I)** lactate, **J**) citrate, and **K**) ribose. Mice with NTshRNA or shPEPCK Colo205 xenografts were injected IP with [U5]-^{13}C glutamine, euthanized 3 hr later and tumors harvested for GC/MS analysis. N=5 ± SD, *p < 0.05.

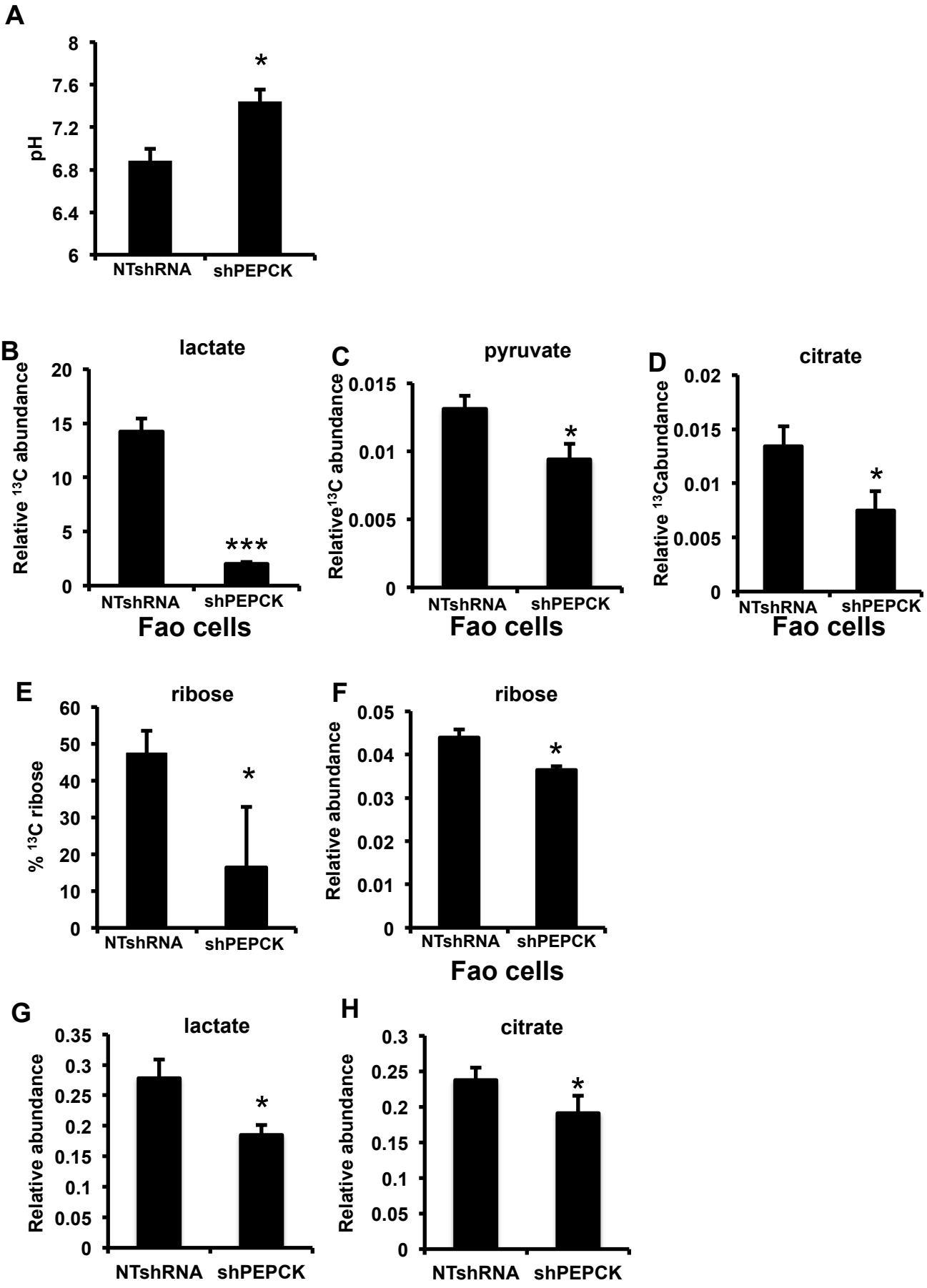
A
pH
8
7.6
7.2
6.8
6.4
6
*
NTshRNA
shPEPCK
B
lactate
Relative 13C abundance
20
15
10
5
0
***
NTshRNA
shPEPCK
Fao cells
C
pyruvate
Relative13C abundance
0.015
0.01
0.005
0
*
NTshRNA
shPEPCK
Fao cells
D
citrate
Relative 13Cabundance
0.02
0.015
0.01
0.005
0
*
NTshRNA
shPEPCK
Fao cells
E
ribose
% 13C ribose
60
50
40
30
20
10
0
*
NTshRNA
shPEPCK
F
ribose
Relative abundance
0.05
0.04
0.03
0.02
0.01
0
*
NTshRNA
shPEPCK
Fao cells
G
lactate
Relative abundance
0.35
0.3
0.25
0.2
0.15
0.1
0.05
0
*
NTshRNA
shPEPCK
H
citrate
Relative abundance
0.3
0.25
0.2
0.15
0.1
0.05
0
*
NTshRNA
shPEPCK

Figure S4, related to Figure 5. PEPCK promotes glucose utilization .

A) pH of media from NTshRNA and shPEPCK Colo205 cells determined using a Nova Bioanalyzer
Relative abundance of ^{13}C labeled **B**) lactate, **C**) pyruvate and **D**) citrate from Fao NTshRNA and shPEPCK cells following labeling with ^{13}C glucose.

E) Fractional labeling of ^{13}C labeled ribose derived from [U6] ^{13}C glucose.

F) Relative abundance of ^{13}C labeled ribose from Fao NTshRNA and shPEPCK cells following labeling with ^{13}C glucose.

N=3 ± SD, *p < 0.05, **p < 0.01, ***p < 0.005.

Mice with NTshRNA or shPEPCK Colo205 xenografts were injected IP with [U6]-^{13}C glucose, euthanized 3 hr later and tumors harvested for GC/MS analysis.

Relative abundance of ^{13}C labeled **G**) lactate and **H**) citrate. Mice with NTshRNA or shPEPCK Colo205 xenografts were injected IP with [U6]-^{13}C glucose, euthanized 3 hr later and tumors harvested for GC/MS analysis. N=5 ± SD, *p < 0.05.

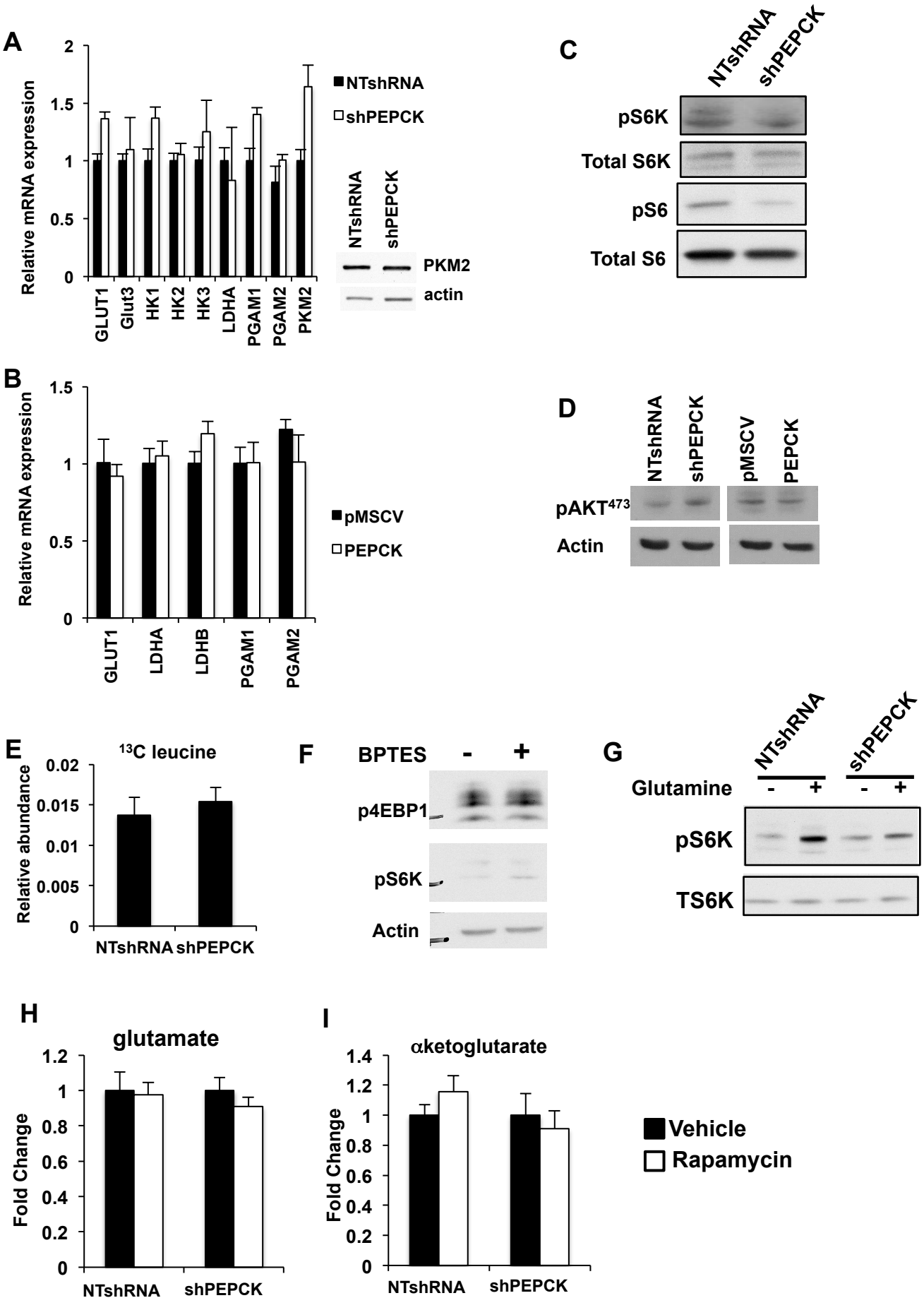
A
Relative mRNA expression
2
1.5
1
0.5
0
GLUT1
Glut3
HK1
HK2
HK3
LDHA
PGAM1
PGAM2
PKM2
NTshRNA
shPEPCK
NTshRNA
shPEPCK
PKM2
actin
B
Relative mRNA expression
1.5
1
0.5
0
GLUT1
LDHA
LDHB
PGAM1
PGAM2
pMSCV
PEPCK
C
NTshRNA
shPEPCK
pS6K
Total S6K
pS6
Total S6
D
NTshRNA
shPEPCK
pMSCV
PEPCK
pAKT473
Actin
E
13C leucine
Relative abundance
0.02
0.015
0.01
0.005
0
NTshRNA shPEPCK
F
BPTES - +
p4EBP1
pS6K
Actin
G
NTshRNA
shPEPCK
Glutamine
- + - +
pS6K
TS6K
H
glutamate
Fold Change
1.2
1
0.8
0.6
0.4
0.2
0
NTshRNA
shPEPCK
I
αketoglutarate
Fold Change
1.4
1.2
1
0.8
0.6
0.4
0.2
0
NTshRNA
shPEPCK
Vehicle
Rapamycin

Figure S5, related to Figure 7. PEPCK promotes glucose utilization via mTORC1 activation.
A and B) PEPCK does not affect glycolytic gene expression. RT-PCR for glycolytic gene expression in **A**) NTshRNA and shPEPCK Colo205 cells or **B**) HT29 cells with pMSCV and PEPCK expression constructs. Inset- western blot for PKM2 expression in Colo205 cells with scrambled shRNA or shPEPCK.
C) Western blot for phosphoS6K, total S6K, phosphoS6 and total S6 from NTshRNA and shPEPCK Colo205 cells.
D) Western blot for phosphoAKT^{473} or actin in Colo205 and HT29 cells with loss or gain of PEPCK.
E) PEPCK does not alter leucine metabolism. Colo205 cells were cultured in $^{13}C_1$ leucine and GC/MS analysis performed for the incorporation of ^{13}C leucine carbons into citrate.
F) Inhibition of glutamine metabolism does not block mTORC1 activity. Colo205 cells were incubated in the presence of 10 μM BPTES overnight. Proteins were harvested and western blot performed for phospho4EBP1, phospoS6K or actin as a loading control.
G) Glutamine is responsible in part for the activation of mTORC1 in PEPCK expressing cells. Cells were cultured as described in Figure 7 and western blotting performed for phosphoS6 kinase and total S6 Kinase.
H and **I**) Rapamycin does affect glutamine utilization. NTshRNA and shPEPCK Colo205 cells were cultured overnight in media containing [U5]-13C glutamine in the absence and presence of 10 nM rapamycin. GC/MS analysis was performed for 13C labeled αketoglutarate and glutamate.
N=3 ± SD